

Detecting Very High Energy Neutrinos by the Telescope Array

Makoto Sasaki* and Masashi Jobashi†

*Institute for Cosmic Ray Research, University of Tokyo,
5-1-5 Kashiwanoha, Kashiwa 277-8582, Japan*

(Dated: March 1, 2002)

We present the potential of the Telescope Array detector for quasi-horizontally downward and upward air showers initiated by Very High Energy Neutrino penetrating the air and the Earth respectively, adopting model predictions for extraterrestrial neutrino fluxes from active galactic nuclei, gamma-ray bursters, the collapse of topological defects, and Z-bursts.

I. INTRODUCTION

The detection of very high energy cosmic neutrinos is important from at least three points of view. First, they can carry astrophysical information about point sources which are optically thick at almost all wavelengths and relics of an early inflationary phase in the history of the universe. Second, the connection between the emission of cosmic nuclei, gamma rays, and neutrinos from astrophysical accelerators is of considerable interest for the solution of the problem of the origin of extragalactic extremely high energy cosmic rays. Third, the final flux of high energy cosmic neutrinos are expected to be almost equally distributed among the three flavors due to vacuum oscillations, provided that neutrinos are produced by distant objects like Gamma Ray Bursters (GRBs) and Active Galactic Nuclei (AGN). The study of oscillation effects on high energy neutrino flux can thus offer the possibility to probe neutrino mixing and distinguish between different mass schemes [1].

Cosmic neutrinos with energies above 10^{16} eV, so far unobserved, are also detectable with the Telescope Array (TA) detector and have great potential as probes of astrophysics and particle physics phenomena. They escape from dense regions of matter and point back to their sources, thereby providing a unique window into the most violent events in the universe. Whatever the sources and mechanisms by which hadrons are accelerated to extremely high energies in the source, and whatever the details of the composition (i.e. pp and/or $p\gamma \rightarrow \pi^\pm$) and subsequent decay of accompanying pions is expected to result in neutrino fluxes through the decay process: $\pi \rightarrow \mu + \nu_\mu \rightarrow e + \nu_e \nu_\mu + \nu_\mu$, leading to the familiar ratio $\nu_\mu/\nu_e = 2$. Observations of cosmic rays with energies beyond the GZK cutoff also raise strong interest in extremely high energy neutrinos [2, 3, 4]. All of new proposals for exotic sources inspired by the super-GZK events can lead to neutrino fluxes well above those guaranteed by the GZK mechanism [5, 6].

A curious coincidence between the energy flow of the highest energy cosmic rays and gamma ray bursts (GRB) suggests a possible common source [7]. Another speculation is that very high energy cosmic rays may be the result of annihilation of topological defects left over from the early universe [8, 9]. The energy scales of such events are of the order of 10^{24} eV (GUT scale). Beyond these ideas is the possibility that the highest energy cosmic rays are evidence for new particle physics or new astrophysics [10]. The super-GZK events also provide motivation for determining whether the photo production mechanism actually occurs in the predicted way. The neutrino fluxes of some representative sources are given in Fig.1. In any case, neutrino induced air-showers can deeply penetrate air mass. The imaging technique using in the TA detector has fairly good advantage to observe the slant depth of deeply penetrating air-shower.

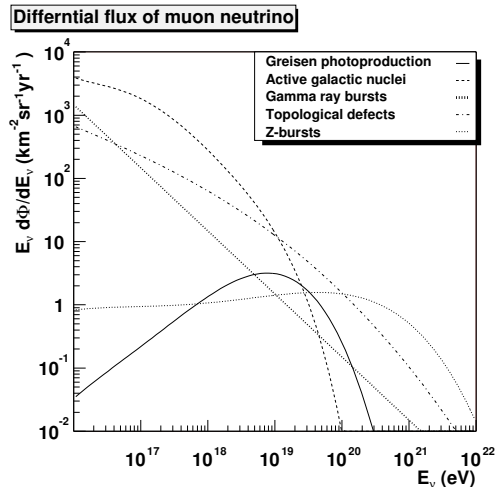


FIG. 1: Differential fluxes of muon neutrinos ($\nu_\mu + \bar{\nu}_\mu$) from Greisen photo production [15](solid), active galactic nuclei [16](long dashed), topological defects [17](short dashed), and Z-bursts [18](dotted).

The recent discovery of near-maximal ν_e - ν_μ and ν_μ - ν_τ mixing [11] has a significant impact on the detection strategy. The proposed astrophysical sources produce predominantly ν_μ with very small admixtures of ν_τ .

*Electronic address: sasaki@icrr.u-tokyo.ac.jp

†Electronic address: jobashi@icrr.u-tokyo.ac.jp

However, these sources are so far away that, even at the high energies of interest here, cosmic neutrino flux at the source, $\nu_e : \nu_\mu : \nu_\tau$ ratio of $1 : 2 : 0$, inevitably oscillates in the three neutrino framework to $1 : 1 : 1$, irrespective of the mixing angle relevant to the solar data.

By looking for upward moving showers from Earth-skimming tau neutrinos, one can test for the existence of neutrino oscillations [12, 13]. Once created in the Earth, a charged lepton loses energy through bremsstrahlung, pair production, and photonuclear interactions. At the Earth's surface with density of about 2.7 g/cm^3 , taus and muons are expected to travel 11 km and 1.5km, respectively, before losing a decade in energy although electrons do not travel at all. Detectable neutrinos therefore skim the Earth at angles approximately 1° above the horizontal and these events are expected to be dominantly showers induced by tau neutrinos.

Another important signature of very high energy tau neutrinos is the “double bang” which they would produce in the atmosphere. The first shower is produced by the original interaction which creates a tau particle and a hadronic shower. This is followed by the decay of the tau which produces the second shower bang. The two bangs are separated by a distance of $\approx 4.9 \text{ km}$ ($E_\tau/10^{17} \text{ eV}$) where E_τ is the energy of the tau converted from the tau neutrino. The decay length is enough measurable with the imaging telescopes in the TA detector.

II. THE TA DETECTOR

The TA detector (Fig.2 and 3) has been designed in order to clarify the mystery of the origin of the highest energy cosmic rays [19, 20]. For this purpose, the detector is required to obtain much more statistics of events than AGASA has done at the rate of one super-GZK event per year. Also it should provide particle identification as well as accurate directional determination of the primary cosmic ray to test the source models at a high confidence level. The basic concept guiding the design is to detect the image of fluorescence light yielded in air showers in a huge effective aperture, from which the longitudinal shower development is reconstructed.

The TA detector consists of 10 observational stations installed on the line in about 30-40km interval as shown in Fig. 2. Each station consists of 40 telescopes with 3m-diameter f/1 mirror system on 2 layers of supports. 256 2-in PMTs mounted on the focal plane are served as pixels of the fluorescence sensor of each telescope. Each PMT covers the visual field which makes $1.1^\circ \times 1.0^\circ$ to be angular aperture. We expect detection rate by the TA detector for the events with the energy exceeding the GZK-cutoff is more abounding than that of AGASA about 30 times, which is similar with that of another detector of the future; Pierre Auger Observatory (AUGER) [21]. Accuracy of determining of the energy and arrival direction for the highest energy event are roughly 25 % and 0.6° respectively.

To keep good visibility, atmospheric transparency, no significant nearby sources of light pollution, and away from main traffic, the detector stations are preferable to install on top of small mountains or hills without sacrificing arrangement in 30-40km interval. We have selected sites in southern part of Utah state, south-west area of Delta. The detector station array is expanded in 200 km square area.

III. NEUTRINOS DEEPLY PENETRATING THE ATMOSPHERE

Neutrinos produce showers in most interactions with the atmosphere which are of different nature depending on the process in consideration. We consider both inelastic charged and neutral current interactions which always produce hadronic showers. In the case of charged current electron neutrino interactions the emerging electron contributes in addition a pure electromagnetic shower carrying a large fraction of the incoming particle energy.

We use new calculations of the cross sections for charged-current and neutral current interactions of neutrinos with nuclei [22, 26], according to the CTEQ4-DIS (deep inelastic scattering) parton distributions [27]. The CTEQ4-DIS parton distributions take account of new information about the parton distributions within the nucleon [28] using more accurate and extensive DIS data than before from New Muon Collaboration (NMC) [29] and DESY ep collider HERA[30, 31], as well as new data from E665[32].

For a neutrino flux dI_ν/dE_ν interacting through a process with differential cross section $d\sigma/dy$, where y is the fraction of the incident particle energy transferred to the target, the event rate for deeply penetrating showers can be obtained by a simple convolution:

$$\text{Rate}[E_{sh} > E_{th}] = N_A \rho_{air} \int_{E_{th}}^{\infty} dE_{sh} \int_0^1 dy \frac{dI_\nu}{dE_\nu}(E_\nu) \frac{d\sigma}{dy}(E_\nu, y) \epsilon(E_{sh}),$$

where N_A is Avogadro's number and ρ_{air} is the air density. The energy integral corresponds to the shower energy E_{sh} which is related to the primary neutrino energy E_ν in a different way depending on the interaction being considered. ϵ is a detector acceptance, a function of shower energy, which corresponds to the volume and solid angle integrals for different shower positions and orientations with respect to the detector. The function is different for showers induced by charged current electron neutrino interactions from those arising in neutral current or muon neutrino interactions. This is because hadronic and electromagnetic showers have differences in the particle distributions functions, particularly for muons. For $(\nu_e + \bar{\nu}_e)N$ charged current interactions, we take the shower energy to be the sum of hadronic and electromagnetic energies, $E_{sh} = E_\nu$. For $(\nu_\mu + \bar{\nu}_\mu)N$ charged current interactions and for neutral current interactions, we take the shower energy to be the hadronic

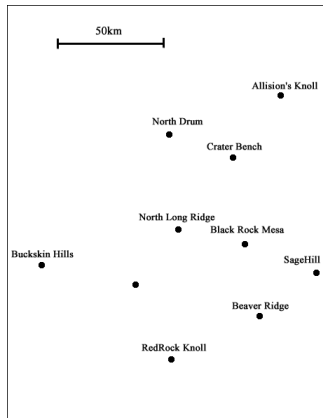


FIG. 2: TA site arrangement.



FIG. 3: TA detector station.

energy, $E_{sh} = yE_\nu$. We use the inelasticity y as a function of E_ν from a reference [22], while $\langle y \rangle \sim 0.25$ does not depend strongly on the primary energy beyond 10^{16} eV in both cases of charged and neutral current interactions.

In the case of ν_τ , we also take into account the decay length of secondary τ , subsequent decay of τ , and another energy deposit into air shower induced by decayed electrons, photons, and hadrons. The tau decay branching fractions and tau polarization effect are reasonably taken into account simply assuming energies of neutral mesons fully contribute to electromagnetic showers. The adopted decay branching fractions and the momentum spectra of the decay with the polarization of ± 1 in the collinear approximation in the laboratory frame are shown in Table I and Fig. 4 respectively. The τ decay length is often long enough and two subsequent energy depositions into air showers can be seen with in the field of view.

TABLE I: Tau decay branching fractions from PDG [39] and used in the simulation for events in TA. The branching fractions in the simulation should include π^0 contributions.

Tau decay modes	PDG B.F. (%)	B.F. (%) in the simulation
$\tau \rightarrow \mu\nu\bar{\nu}$	17.37 ± 0.07	17
$\tau \rightarrow e\nu\bar{\nu}$	17.83 ± 0.06	18
$\tau \rightarrow \pi(K)\nu$	11.79 ± 0.12	13
$\tau \rightarrow \rho\nu$	25.40 ± 0.14	37 (≥ 1 neutral)
$\tau \rightarrow a_1\nu$	9.49 ± 0.11	15 (all 3-prongs)
$\tau \rightarrow hhh \geq \pi^0\nu$	4.49 ± 0.08	

Each simulation for a given primary cosmic ray (electron neutrino, muon neutrino, tau neutrinos, or proton) was performed at fixed energy. The shower energy of neutrinos depends on the generation as described above. For each shower energy, the mean depth of proton shower maximum was determined from simulations[33]. For each primary particle at each energy, the mean of the interaction length X_1 was determined from the above interaction cross sections of neutrinos with nuclei or that of

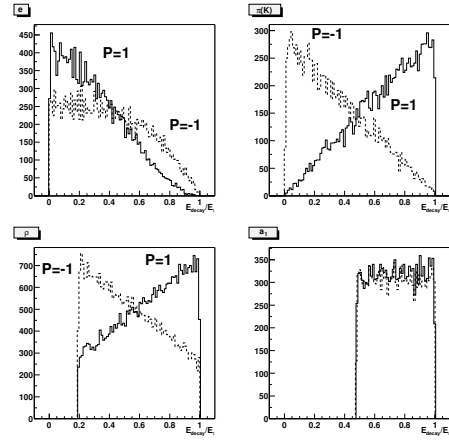


FIG. 4: Distributions in visible decay energy divided by E_τ corresponding to values of tau polarization ± 1 for $\tau \rightarrow e\nu\bar{\nu}$, $\tau \rightarrow \pi(K)\nu$, $\tau \rightarrow \rho\nu$, and $\tau \rightarrow a_1\nu$.

protons, $83.1(E/\text{GeV})^{-0.052} \text{ g/cm}^2$ [34]. The shower energy determines the shower size at maximum, N_{max} [35]. Given N_{max} , X_{max} , and X_1 , the complete longitudinal profile was described by the Gaisser-Hillas function[25]. The NKG lateral distribution function[36, 37] normalized with the Gaisser parameterization has been used for the total number of electrons and positrons in hadronic (electromagnetic) cascade showers to determine the location where fluorescence lights are produced. We took into account the fluctuations of the first interaction depth, impact point, and directional angles of air shower cores with appropriate distributions but not air shower size fluctuations.

The light yield arriving at the detector site is calculated. Rayleigh and Mie scattering processes are simulated, with full account taken of the spectral characteristics of the light. The isotropically emitted fluorescence light, as well as direct and scattered Cerenkov light, is

propagated. Night sky background noise is added to the signal. All processes that affect to overall optical efficiency; mirror area and reflectivity, optical filter transmission, PMT quantum efficiency factors are folded with the light spectrum to give the photoelectron yield in each PMT, due to signal and noise.

A “fired” PMT is defined to require that its instantaneous photoelectron current is greater than the 4σ noise level of the night sky background. We preselected events if at least one of 10 eyes contains at least 6 firing PMTs. To ensure track quality, we cut events of which shower maximums are not viewed by any eye. Finally to reject proton background events, we selected only events with $X_{max} > 1700 \text{ g/cm}^2$. We obtained the detector aperture corresponding the above selection cuts and calculated them into the acceptances multiplying the appropriate interaction length of neutrino with nucleon. Figure 5 shows shower slant depth distributions from Monte Carlo simulations by which neutrino events can be distinguished from proton events. The results are shown in Fig. 6 for both electron, muon, and tau neutrinos as a function of the primary energy. The acceptances of TA for high-energy neutrinos deeply penetrating air are turned out to be fairly competitive with those of IceCube and AUGER [22, 23, 24] in lower and higher energy regions respectively even if we take into account the 10 % duty factor of TA.

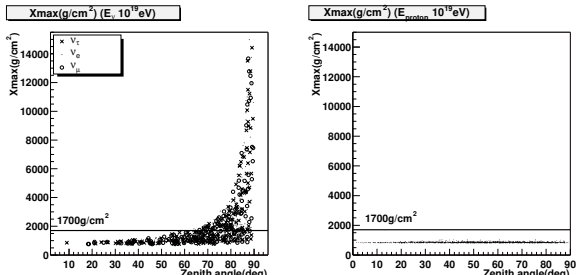


FIG. 5: Shower slant depth distributions for neutrino (left) and proton (right) induced events with the energies of 10^{19} eV from Monte Carlo simulations showing the cut of 1700 g/cm^2 , by which neutrino events can be distinguished from proton events.

IV. EARTH-SKIMMING TAU NEUTRINOS

Very high energy neutrinos penetrate the Earth and convert to charged leptons in the Earth, and these leptons then run in the Earth. A schematic picture of the events to be considered is shown in Fig. 7. We define the critical angle θ_c satisfying that the chord thickness at nadir angle θ_c corresponds to the charged current interaction length $L_{CC}^\nu(E_\nu)$ determined by the interaction cross section for a neutrino traveling with energy E_ν . For nadir angle smaller than θ_c , neutrinos are shadowed by the Earth and for larger nadir angles,

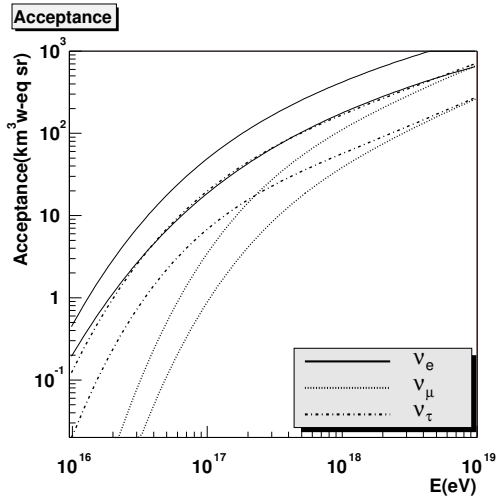


FIG. 6: Acceptance of the TA detector (10 stations) to neutrino induced air shower. Volume units are km^3 of water equivalent. The higher and lower curves correspond to events after preselection and proton rejection cuts respectively.

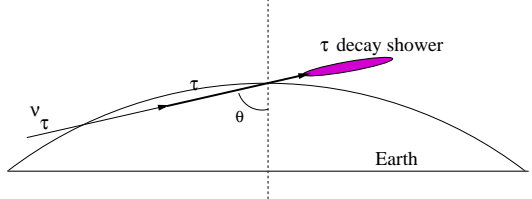


FIG. 7: A schematic picture of the Earth-skimming tau neutrino events.

they rarely interact to produce charged leptons. Table II shows charged current cross sections, interaction lengths, and 90° minus corresponding critical angles at various neutrino energies. For neutrino energies above 10^{17} eV , we see that $90^\circ - \theta_c$ is small and both the neutrinos and the created leptons travel essentially horizontally.

TABLE II: Charged current cross sections, interaction lengths and 90° minus critical angle θ_c (see text) for νN interactions for the CTEQ-DIS distributions [22].

E_ν (eV)	σ_{CC}^ν (cm ²)	L_{CC}^ν (g/cm ²)	$90^\circ - \theta_c$ (°)
10^{16}	1.76×10^{-33}	9.44×10^8	16
10^{17}	4.78×10^{-33}	3.47×10^8	5.9
10^{18}	1.23×10^{-32}	1.35×10^8	2.3
10^{19}	3.01×10^{-32}	5.52×10^7	0.89
10^{20}	7.06×10^{-32}	2.35×10^7	0.35

Once created, a charged lepton loses energy through bremsstrahlung, pair production, and photonuclear interactions. Electrons lose their energy too quickly in the Earth to emerge to be detected by fluorescence. Assum-

ing that the lepton loses energy uniformly and continuously, its energy loss can be parametrized by: $dE_l/dz = -\beta_l \rho$, where the Earth density can be simplified to be 2.65 g/cm^3 uniformly for small nadir angle. The values of β_l are given by: $\beta_\mu \sim 6.0 \times 10^{-6} \text{ cm}^2/\text{g}$, $\beta_\tau \sim 0.8 \times 10^{-6} \text{ cm}^2/\text{g}$, for the energies of interest here [38]. In consequence, at the Earth's surface, muons and taus can travel 1.5 km and 11 km, respectively, before losing a decade in energy. Therefore, the tau neutrinos contribute dominantly to Earth-skimming events observed above the Earth's surface. Figure 8-9 show distributions on the plane of energy E_τ and 90° minus nadir angle of taus that exit the Earth from the primary neutrinos with energies of 10^{19} eV and 10^{17} eV .

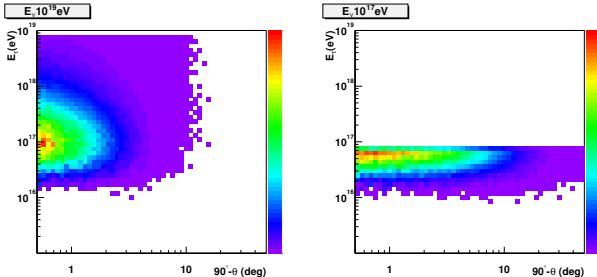


FIG. 8: Distribution on the plane of energy E_τ and 90° minus nadir angle θ of tau that exits the Earth in the case of the primary neutrino energy of 10^{19} eV .

FIG. 9: Same but the primary neutrino energy of 10^{17} eV .

The survival probability P_{svv} for a tau losing energy as it moves through the Earth is described by the energy loss dE_τ/dz as above shown and

$$\frac{dP_{svv}}{dz} = -\frac{P_{svv}}{c\tau_\tau E_\tau/m_\tau}$$

where c is the speed of light, and m_τ and τ_τ are tau's rest mass and lifetime, respectively. These are simply solved and the survival probability is given in:

$$P_{svv} = \exp \left[\frac{m_\tau}{c\tau_\tau \beta_\tau \rho} \left(\frac{1}{E_\nu} - \frac{1}{E_\tau} \right) \right]$$

For taus, this factor plays a significant role.

On the other hand, the flux of survived taus with energy $E_{min} < E_\tau < E_{max}$ is:

$$\Phi_\tau = \frac{\ln(E_{max}/E_{min})}{2R\beta_\tau \rho} \Phi_\nu ,$$

where Φ_ν is the flux of neutrinos. As a result, the flux in any given decade in tau energy is $\Phi_\tau = 8.5 \times 10^{-4} \Phi_\nu$, that is, 1 in every 1200 neutrinos skims the Earth and emerges as a tau with the required energy [12]. This remarkably simple and robust statement is quite useful because it is independent of the neutrino energy and microscopic

details. We have examined our Monte Carlo simulation results by comparing with this analytic estimate.

The tau decay length is given in: $L_\tau = c\tau_\tau(E_\tau/m_\tau) \approx 4.9 \text{ km}(E_\tau/10^{17} \text{ eV})$, using the lifetime of $c\tau_\tau = 87.11 \mu\text{m}$ the tau mass of $m_\tau = 1777.03 \text{ MeV}$ from PDG [39]. The treatments for tau decays, polarization, and so on are same as described in the previous section. Effective detection apertures and acceptances have been estimated for Earth-skimming tau events changing the neutrino energies from the detailed Monte Carlo simulation. Figure 10 shows the effective detection acceptances using only one TA station.

Acceptance of Skimming Tau Neutrino

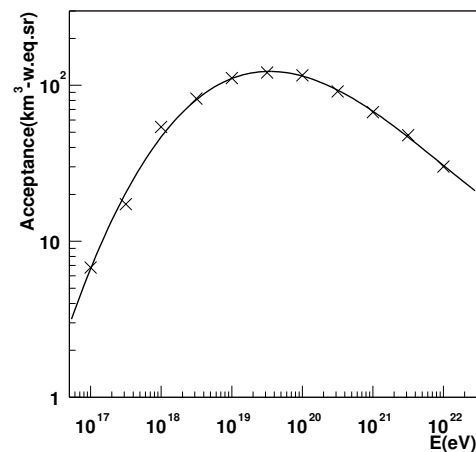


FIG. 10: Detection acceptance estimate for Earth-skimming tau leptons through their decays to electromagnetic or/and hadronic air showers with only one TA detector station.

V. DETECTION EVENT RATES

There is a model that assumes shock acceleration in the AGN cores and predicts relatively flat fluxes up to energies of about 10^{15} eV . The GeV to TeV gamma ray emission is observed from AGN corresponds to the blazar class. Most recent models for the proton blazars site the acceleration in the jets themselves. We use the prediction of [16], which illustrates that the emitted neutrinos may extend well into the EeV region. Annual event rates have been calculated in the TA detector for neutrino induced air showers with fluxes from GRB model [7], and Greisen neutrino [15] models as well as from AGN-jet [16], assuming the duty cycle of 10%, which are shown in Table III. The testability for the bottom-up scenario models is statistically nice even only through shower events deeply penetrating the air.

Also we compare the detectability for Earth-skimming tau neutrino events with those for the downward events above described. Table IV lists annual event rates for neutrino induced air-showers from various models including top-down scenario sources through shower events

deeply penetrating the air and Earth-skimming events. The duty factor of 10 % is assumed as usual. As a result, the enhancement of statistics using Earth-skimming events is significant particularly in ultra-high energy region. Hence it is feasible to test the top-down scenario models like topological defects and Z-bursts in a statistically significant way through both of downward and upward neutrino-induced air-shower events in complementary energy regions respectively.

TABLE III: Annual event rates in the TA detector for neutrino induced air showers with fluxes from AGN-jet [16], GRB model[7], and Greisen neutrino [15] models (see text). The duty factor of 10% was assumed.

	CC ν_e	CC ν_μ	CC ν_τ	NC	Total
AGN (yr^{-1})	13	2.5	5.7	4.3	25.5
GRB (yr^{-1})	1.1	0.3	0.5	0.4	2.3
Greisen (yr^{-1})	0.96	0.37	0.59	0.63	2.6

TABLE IV: Annual event rates of Earth-skimming tau neutrinos from model sources with ten detector stations.

	Greisen	AGN	GRB	TD	Z-burst
ν DPS (yr^{-1})	2.6	25.5	2.3	~ 0	~ 0
Earth skimming ν (yr^{-1})	0.7	14.5	1.2	5.5	0.6
Total event rates (yr^{-1})	3.3	40.0	3.5	5.5	0.6

VI. CONCLUSIONS

The next generation cosmic ray detectors like AUGER and TA can have target volumes of atmosphere, which are so competitive with or more than that of IceCube that annual detection rate assuming AGN-jet proton acceleration models are statistically sizable [24][23]. TA using air fluorescence technique is advanced for primary neutrino identification discriminating from proton induced air showers. Recently a novel detection strategy for Earth-skimming extremely high energy neutrinos has been quantitatively proposed that improvements are significant at the TA detector comparing to that for down-going neutrino detection [12], encouragingly, extremely high energy cosmic neutrino sources except for AGN-jets like Greisen photo production [15], topological defects [17], long-lived super heavy particles, and Z-bursts [18] may be experimentally tested well with TA.

VII. ACKNOWLEDGMENTS

I am indebted to my colleagues in the TA Collaboration, especially those who have contributed to the TA Design Report, for assistance in the preparation of this paper. I would like to special acknowledge the contributions of Prof. T.Matsuda and Prof. C.Fukunaga for useful discussions.

[1] H. Athar, M. Jezabek and O. Yasuda, Phys. Rev. D62 (2000) 103007.
[2] M. Takeda et al., Phys. Rev. Lett. **81** (1998) 1163.
[3] J.D. Bird et al., Phys. Rev. Lett. **71** (1993) 3401.
[4] B.N. Afanasiev et al., Proc. 24th ICRC, Roma, **2** (1995) 756.
[5] K. Greisen, Phys. Rev. Lett. **16** (1966) 748.
[6] G.T. Zatsepin and V.A. Kuzmin, JETP Letters **4** (1966) 78.
[7] E. Waxman, Phys. Rev. Lett. **75** (1995) 386.
[8] C.T. Hill, D.N. Schramm and T.P. Walker, Phys. Rev. D**36** (1987) 1007.
[9] P. Bhattacharjee, C.T. Hill and D.N. Schramm, Phys. Rev. Lett. **69** (1992) 567.
[10] T. J. Weiler, Astropart. Phys. **11**, 303 (1999).
[11] S. Fukuda et al (Super-Kamiokande Collaboration), Phys. Rev. Lett. **86** (2001) 5656.
[12] J.L. Feng, P. Fisher, F. Wilczek, and T.M. Yu: hep-ph/0105067.
[13] D. Fargion, B. Mele, and A. Salis, Astrophys. J. **517**, (1999) 725.
[14] J.G. Learned and S. Pakvasa, Astropart. Phys. **3**, (1994) 267.
[15] F.W. Stecker: Astrphys. J. **228** (1979) 919.
[16] K. Mannheim, Astropart. Phys. **3** (1995) 295.
[17] G. Sigl, et al., Phys. Rev. D**59** (1999) 043504.
[18] S. Yoshida, G. Sigl and S. Lee, Phys. Rev. Lett. **81** (1998) 5505.
[19] M. Sasaki, Proc. 25th ICRC, **5**, 369 (Durban, 1997).
[20] The Telescope Array Project: Design Report, <http://www-ta.icrr.u-tokyo.ac.jp>; M. Sasaki, Proc. of the EHECR2001, ICRR-Report-481-2001-11 (2001).
[21] The Pierre Auger Project: Design Report, 2nd ed. March 1997, <http://www.auger.org/>.
[22] R. Gandhi, C. Quigg, M. H. Reno, and I. Sarcevic, Astropart. Phys. **5** (1996) 81.
[23] M. Sasaki: Proc. the 1st workshop on *Neutrino Oscillations and their Origin*, (2000) 79.
[24] K.S. Capelle, J.W. Cronin, G. Parente and E. Zas: Astropart. Phys. **8** (1998) 321.
[25] T. K. Gaisser and A. M. Hillas, Proc. 15th ICRC (Plovdiv) **7** (1977) 353.
[26] R. Gandhi, C. Quigg, M. H. Reno, and I. Sarcevic, Phys. Rev. D **58**, 093009 (1998).
[27] CTEQ Collaboration, H. L. Lai *et al.*, Phys. Rev. D **55** 1280 (1997).
[28] C. Quigg, FERMILAB-CONF-97/158-T.
[29] NMC, M. Arneodo *et al.*, Phys. Lett. B **36** 471 (1995).
[30] H1 Collaboration, S. Aid *et al.*, Nucl. Phys. B **439** 471 (1995); Nucl. Phys. B **470** 3 (1996).
[31] ZEUS Collaboration, M. Derrick *et al.*, Z. Phys. C **65** 379 (1995).
[32] E665 Collaboration, M. R. Adams *et al.*, Phys. Rev. D **54**, 3006 (1996).
[33] T. K. Gaisser *et al.*, Phys. Rev. D **47**, 1919 (1993).
[34] M. Honda *et al.*, Phys. Rev. Lett., **70**, 525 (1993).

- [35] R. M. Baltrusitis *et al.*, Proc. 19th ICRC, La Jolla, **7** (1985) 159.
- [36] K. Kamata and J. Nishimura, Prog. Theor. Phys. Suppl. **6**, 93 (1958).
- [37] K. Greisen, Prog. Cosmic Ray Physics **3**, 1 (1956).
- [38] P. Lipari and T. Stanev, Phys. Rev. **D44** 3543 (1991).
- [39] Particle Data Group (D.E. Groom *et al.*) Eur. Phys. J. **C15**, 1-878 (2000).